Research paper

Compounds targeting YadC of uropathogenic *Escherichia coli* and its host receptor annexin A2 decrease bacterial colonization in bladder

Xiao Li[a,1], Geng Pei[a,1], Lisong Zhang[b], Yang Cao[c], Jingyu Wang[a], Lu Yu[a], Wei Dianjun[c], Shan Gao[b], Zhi-Song Zhang[b], Zhi Yao[a,d], Quan Wang[a,*]

[a] *Department of Immunology, Key Laboratory of Immune Microenvironment and Disease of the Educational Ministry of China, Tianjin Key Laboratory of Cellular and Molecular Immunology, School of Basic Medical Sciences, Tianjin Medical University, 22 Qixiangtai Road, Heping District, Tianjin 300070, China*
[b] *State Key Laboratory of Medicinal Chemical Biology and College of Pharmacy, Collaborative Innovation Center for Biotherapy, and Tianjin Key Laboratory of Molecular Drug Research, Nankai University, Tianjin 300350, China*
[c] *Department of Clinical Laboratory, The Second Hospital of Tianjin Medical University, Tianjin 300211, China*
[d] *2011 Collaborative Innovation Center of Tianjin for Medical Epigenetics, Tianjin Medical University, Tianjin 300070, China*

A R T I C L E   I N F O

A B S T R A C T

Background: Uropathogenic *Escherichia coli* (UPEC) is the leading cause of urinary tract infections (UTIs), and fimbrial tip adhesins, play important roles in UPEC colonization. Few fimbrial tip adhesins and their receptors on host cells, which have the potential to be the therapeutic targets, have been identified.
Methods: the UPEC wild-type strain CFT073, ΔyadC and the complemented strain were used to perform assays in vitro and in vivo. The effects of D-xylose targeting YadC on UPEC colonization were evaluated. A YadC receptor was identified by far-western blotting, LC-MS/MS and co-immunoprecipation. The effects of compounds targeting the receptor on UPEC colonization were tested.
Findings: YadC was investigated for its mediation of UPEC adhesion and invasion to bladder epithelial cells in vitro; and its promotion of UPEC colonization in bladder in vivo. D-xylose, targeting YadC, showed prophylactic and therapeutic effects on UPEC colonization. Annexin A2 (ANXA2) was identified as a YadC receptor, involved in UPEC infection. ANXA2 inhibitors attenuated UPEC infections. The *yadC* gene was widely present in UPEC clinical isolates and phylogenetic analysis of *yadC* was performed.
Interpretation: YadC and its receptor ANXA2 play important roles in UPEC colonization in bladder, leading to novel treatment strategies targeting YadC or ANXA2 for acute UTIs.

1. Introduction

Urinary tract infections (UTIs), mainly caused by Uropathogenic *Escherichia coli* (UPEC), are one of the most common bacterial infections worldwide, which induce cystitis, pyelonephritis, and prostatitis in humans, and cause serious economic and medical burdens [1, 2] UPEC colonization in the urinary tract is important for its pathogenesis, while adhesion and invasion to epithelial cells are necessary for effective colonization [3, 4]. Therefore, inhibiting UPEC colonization during UTIs is an effective strategy to prevent related diseases.

Many kinds of fimbriae have been found in UPEC strains, with eight to thirteen fimbrial gene clusters present in each isolate [5]. Fimbriae mediate diverse functions, such as adherence and biofilm formation. For example, type 1 fimbriae stimulates UPEC infection of bladder epithelial cells [6], and P fimbriae enhances UPEC colonization in the kidney [7]. Fimbrial tip adhesins recognize specific receptors on host cells to promote bacterial adhesion and invasion [8]. FimH and PapG have been identified as the respective tip adhesin for Type 1 and P fimbriae [7, 9, 10].

UTIs are usually treated with antibiotics; however, UPEC strains can be found in the urinary tract for weeks after antibiotic treatment, and multidrug-resistant strains are increasing, highlighting the importance of developing alternative treatment strategies [11–13]. Some anti-adhesion agents, such as mannosides for type 1 fimbriae

* Corresponding author.
E-mail address: wangquan@tmu.edu.cn (Q. Wang).
[1] These authors contributed equally.

Research in context

Evidence before this study

Fimbrial tip adhesins recognizing specific receptors on host cells are important for UPEC to colonize in the urinary tract. There are 8 to 13 fimbrial gene clusters present in each UPEC isolate, and few tip adhesins and their host receptors have been identified.

Added value of this study

YadC, the tip adhesin of Yad fimbriae, was investigated to promote UPEC colonization in bladder during acute UTIs. ANXA2 on bladder cells was identified as a YadC receptor, involved in UPEC infection. Compounds targeting YadC or ANXA2 reduced UPEC colonization in bladder during acute UTIs.

Implications of all the available evidence

UTIs are usually treated with antibiotics, and multidrug-resistant strains are rising. Agents targeting the UPEC factors or their host receptors important for the pathogenicity could lead to novel non-antibiotic strategies to treat UTIs.

and globotetraose for P fimbriae, have been developed as non-antibiotic therapies for UTIs [14, 15]. Identification of the other adhesins that are important for UPEC infections and the corresponding anti-adhesion agents could lead to novel strategies to treat UTIs.

Yad fimbriae is frequently found in UPEC [5, 16]. Yad fimbriae plays a role in avian pathogenic *E. coli* pathogenicity [17, 18] and participates in binding to bladder epithelial cells and biofilm formation [19]. YadC was identified as a potential tip adhesin of Yad fimbriae [20].

Annexin A2 (ANXA2) is widely distributed in various cells, including endothelial cells, monocytes, and epithelial cells, and is involved in many biochemical processes such as cell proliferation, endocytosis, autophagy, and membrane trafficking [21−24]. ANXA2 can reversibly bind to negatively charged membrane phospholipids in a calcium-dependent manner [25, 26], and localizes on the membrane mainly as a stable heterotetramer, which comprises two molecules each of ANXA2 and p11 (S100A10) to form the ANXA2/p11 complex (A2t). S100A10 is a member of the S100 family of EF hand-type Ca^{2+}-binding proteins, intracellular S100A10 participates in the trafficking of several proteins, including ANXA2, to the plasma membrane. In the complex, ANXA2 may protect S100A10 from being rapidly polyubiquitinated and degraded, and S100A10 increases the Ca^{2+} sensitivity of ANXA2 and its capacity to bind membranes and F-actin [27]. ANXA2 was identified as a potential receptor for *Pseudomonas aeruginosa* and viruses [28, 29], and was reported to be involved in bacterial and viral infections of epithelial cells [30−32]. However, the role of ANXA2 in UPEC infection has not been reported.

In the present study, YadC was identified to play an important role in UPEC adhesion and invasion to bladder cells and colonization during acute cystitis. D-xylose targeting YadC had the potential to prevent and treat UPEC infections. ANXA2 was identified as a YadC receptor involved in UPEC infection, and ANXA2 inhibitors showed the potential to treat UPEC infections.

2. Materials and methods

2.1. Cell lines, bacterial strains, and plasmids

The sources of the cell lines are as follows: 5637 (ATCC HTB-9, RRID: CVCL_0126), T24 (ATCC HTB-4, RRID: CVCL_0554). The bacterial strains and plasmids used are listed in Table S1. Bacterial strains were grown at

37 °C in Luria-Bertani (LB) broth and on LB agar plates for 12 h, with the appropriate antibiotics when required in the following concentration: chloramphenicol at 25 μg/ml; kanamycin at 50 μg/ml; and tetracycline at 10 μg/ml. The $\Delta yadC$ and $\Delta fimA$ strains were generated by substitution of *yadC* with a *cat* gene or *fimA* with a *kan* gene respectively using the lambda red recombination system [33]. To construct the complemented strains ($\Delta yadC$ *p-yadC* and $\Delta fimA\Delta yadC$ *p-yadC*), *yadC* was amplified by PCR, cloned into pACYC184, and transformed into the $\Delta yadC$ or $\Delta fimA\Delta yadC$ strains. To get HA and FLAG-tagged YadC protein, the *yadC* of CFT073 was amplified by PCR and cloned into pET-28a (+) and then transformed into *E. coli* BL21. The cDNA encoding ANXA2 was amplified from 5637 cells cDNA and cloned into pET-28a (+) to produce the ANXA2 recombinant protein.

2.2. Adhesion and invasion assays

About 10^5 cells were grown in 24-well plates until confluence at 37 °C in 5% CO_2, and then incubated with bacteria that were grown overnight at 37 °C at the indicated multiplicity of infection (MOI). To block type 1 fimbriae, 1% mannose was used simultaneously with infection. Plates were centrifuged at 600 × g for 5 min to facilitate bacterial contact with the host cell monolayer. One hour after incubation at 37 °C in 5% CO_2, cell monolayers were washed five times with PBS and digested by 500 μl trypsin for 5 min at room temperature. Then 500 μl PBS was added into each well for 10 min. Adherent bacteria were enumerated by plating serial dilutions on LB agar plates. The cells were vigorously washed and lysed with 1 ml 0.2% Triton X-100 for 15 min, and total infected bacteria were enumerated by plating serial lysate dilutions on LB agar plates. For invasion assays, after the initial 1 h incubation, the cells were washed three times with PBS and treated with 100 μg/ml gentamicin for 1 h to kill extracellular bacteria. Then cells were washed three times with PBS, lysed with 1 ml of 0.2% Triton X-100 for 15 min, and lysate dilutions were plated on LB agar plates to enumerate the intracellular bacteria.

2.3. Immunofluorescence analysis of cells

Cells were grown in a LAB-TEK glass 4-well chamber slide and incubated overnight at 37 °C in 5% CO_2. Cells were washed with PBS and infected with bacteria grown overnight at 37 °C for 2 h, washed with PBS, fixed with 4% paraformaldehyde for 30 min and permeabilized with 0.5% Triton X-100 for 15 min. Then cells were blocked with 3% bovine serum albumin (BSA) containing 10% goat serum for 1 h at room temperature, incubated with *E. coli* LPS antibody (Abcam, Cambridge, UK, ab 35654, 1:200, RRID: AB_732222) in blocking buffer overnight at 4 °C. After that, cells were washed five times with PBS, and incubated with Alexa Fluor 488-labeled secondary antibody (Proteintech, Chicago, IL, USA, 1:200) for 1 h at room temperature. Then, 100 nM Rhodamine Phalloidin (Cytoskeleton, Denver, CO, USA) in PBS was used to label F-actin, and the nuclei were counterstained with DAPI. For colocalization of ANXA2 with HA-YadC, 5637 cells were incubated with HA-YadC protein or PBS for 8 h, and antibodies specific for the HA tag (Cell Signaling Technology, Danvers, MA, USA, 2367S, 1:200, RRID: AB_10691311) and ANXA2 (Proteintech, 11256-1-AP, 1:200, RRID: AB_2057311) were used. Images were captured using a confocal fluorescence microscope (FV1000-D, Olympus, Tokyo, Japan). For colocalization of ANXA2 with bacteria, 5637 cells were infected with CFT073 which were grown overnight at 37 °C for 1 h, and antibodies specific for *E. coli* LPS antibody (Abcam, ab 35654, 1:200) and ANXA2 (Proteintech, 11256-1-AP, 1:200) were used. Images were captured using a confocal fluorescence microscope (TCS-SP8, Leica, Germany).

2.4. Motility assay

Bacteria were grown overnight at 37 °C in LB broth, then cultures of each strain were stabbed into the center of soft agar plates (0.3%

agar). The diameter of motility was measured after incubation for 24 h at 30 °C.

2.5. Hemagglutination (HA) assay

Bacteria were grown at 37 °C in LB broth and harvested by centrifugation (4000 × g, 5 min). The pellets were resuspended in PBS to an initial suspension of 10^{10} CFU/ml and serially diluted 2 folds in microtiter wells and then mixed with an equal volume of a 3% (v/v) guinea pig erythrocytes in the absence or presence of 1% mannose. The hemagglutination was monitored visually after 2 h of incubation at 4 °C, the agglutination titer was recorded as the most diluted bacterial sample giving a positive aggregation reaction.

2.6. Mouse model of acute UTIs

Female C57BL/6J mice, aged 6−8 weeks, were purchased from the Academy of Military Medical Science (Beijing, China) and randomly divided into different groups. All animal experiments were performed according to the standards in the Guide for the Care and Use of Laboratory Animals (Institute of Laboratory Animal Resources of National Research Council, United States). All mouse studies were approved by the Animal Ethics Committee of Tianjin Medical University and Tianjin Institute of Pharmaceutical Research New Drug Evaluation Co. Ltd (IACUC number: 2017071902), Tianjin, China. We made every effort to minimize animal suffering and to reduce the number of animals used. The model of urinary tract infection was established as previously described [34]. Bacterial strains were grown statically in LB at 37 °C overnight. These cultures were spun at room temperature for 5 min at 5000 × g, resuspended in PBS to dilute to approximately 2 to 4 × 10^9 CFU/ml. After deeply anesthetized with 1.5% pentobarbital sodium, the mice were inoculated with 50 μl of this suspension (~1 to 2 × 10^8 CFU) into the bladder via transurethral catheterization and sacrificed at 12 and 24 h post infection (hpi). Their bladders were removed aseptically, homogenized in 1 ml of PBS containing 0.025% Triton X-100, serially diluted and plated on LB agar plates for enumeration. Bladders were also used for immunofluorescence analysis or H&E staining.

2.7. Immunofluorescence analysis of tissues

Bladders were aseptically harvested, embedded in OCT compound with liquid nitrogen. Frozen sections (5 μm) were cut and air-dried at room temperature for 20 min and fixed with cold acetone for 10 min. The tissues were then immediately submerged in methanol for 20 min and 3% hydrogen peroxide in methanol for 10 min. After rehydration in PBS, sections were blocked with 5% BSA for 1 h, incubated with *E. coli* antibody (Abcam, ab 13627, 1:200, RRID: AB_30051) and Uroplakin Ⅲ antibody (Abcam, ab 187299, 1:200) or Annexin A2 antibody (Proteintech, 11256-1-AP, 1:200, RRID: AB_2057311) in blocking buffer overnight at 4 °C. After that, coverslips were washed five times with PBS, and incubated with Alexa FITC/594-labeled secondary antibody (Proteintech, 1:200) for 1 h. Finally, the tissue sections were counterstained with DAPI for nuclei visualization. Images were acquired using an IX73 fluorescent microscope (Olympus).

2.8. D-xylose treatment

Cell infected with bacteria were performed as described above with or without 0.5 mg/ml D-xylose, after 1 h of infection at 37 °C in 5% CO_2, the adhered and invaded bacteria were enumerated. D-xylose was diluted in PBS and administered to 6−8 week-old C57BL/6J mice at a dose of 100 mg/kg, and mouse urine was collected at different time points after the oral gavage to detect urine D-xylose concentrations as described previously [35]. Developer solution

(5 ml, 0.5 g of phloroglucinol in 10 ml of glacial acetic acid and 6 ml of concentrated hydrochloric acid) were added to 50 μl of mice urine or xylose standard solutions, mixed well, and reacted for 10 min at 100 °C, then cooled to room temperature. The absorbance was then read at 550 nm.

To evaluate the prophylactic effect, one dose of D-xylose was given via oral gavage 30 min before transurethral inoculation with CFT073 (10^8 CFU). The mice were sacrificed and their bladders were processed for analysis of viable bacteria at 3 hpi. To evaluate the therapeutic effect, D-xylose was given by gavage 3 h after CFT073 infections, and mice were sacrificed and the bladder bacteria titers were enumerated at 4 h after treatment.

2.9. Protein purification

Expression of YadC and ANXA2 were performed in *E. coli* BL21 (DE3) and Rosetta (DE3), respectively. Bacteria were cultivated at 37 °C until an OD_{600} of 0.6 to 0.8, inducted with 0.1 mM IPTG and incubated at 30 °C for 6 h (for YadC) or with 0.5 mM IPTG and incubated at 37 °C for 4 h (for ANXA2). Cultured bacteria were harvested by centrifugation (8000 × g for 5 min at 4 °C), and the proteins were purified using the Ni-NTA Purification System (GenScript, Nanjing, China), washed with 50 mM washing buffer, and eluted with 250 mM imidazole. Elution products were pooled, dialyzed and subsequently concentrated to an appropriate volume. The final protein concentration was determined using a BCA Protein Assay Kit (23225, Thermo Scientific, Waltham, MA, USA).

2.10. Far-western blotting and LC-MS/MS analysis

Far-western blotting was performed as previously described [36]. Membrane proteins were extracted using a Membrane and Cytosol Protein Extraction Kit (Beyotime Biotechnology, Shanghai, China) according to the manufacturer's protocol. Samples were separated by SDS-PAGE and transferred to PVDF membrane (Merck Millipore, Darmstadt, Germany). Membranes were blocked in 5% skim milk in TBST buffer for 2 h. Purified HA-tagged YadC or vector protein were added at a concentration of 30 μg/ml and incubated for another 2.5 h at room temperature. After washing five times, the membrane was incubated with anti-HA antibody (CST, C29F4, 1:1000, RRID: AB_1549585) overnight at 4 °C and then incubated with HRP-conjugated anti-Rabbit IgG (Sigma-Aldrich, 1:10000) after washing five times.

The differential protein bands were identified by LC-MS/MS, performed using a nanoLC-LTQ-Orbitrap XL mass spectrometer (Thermo, San Jose, CA, USA) coupled with an Eksigent nano LC 1D plus HPLC system in Majorbio (Shanghai, China). Tryptic peptides were fully enzymatically digested and ionized using nano electrospray ionization. Data were analyzed using a full-scan mass spectrum (300 to 1800 m/z). Finally, Proteome Discoverer (version 1.4.0.288, Thermo Scientific) was used to analyze the MS data.

2.11. Immunoprecipitation (IP) assays

Purified FLAG-YadC protein was added to 5637 cells and incubated for 12 h. The cells were then lysed with lysis buffer (0.2 mM EDTA, 50 mM Tris-HCl (pH7.4), 150 mM NaCl, 1% NP-40). Whole cell lysates were incubated with anti-FLAG M2 beads (A2220, Sigma-Aldrich) for 12 h at 4 °C for FLAG-tagged protein IP. For ANXA2 protein IP, cell lysates were incubated with anti-ANXA2 antibody (Proteintech, 60051-1-Ig) for 12 h at 4 °C, and then incubated with Protein A/G agarose (Thermo Fisher, 20241) for 2 h at 4 °C. Normal Mouse IgG (CST, 3420S, RRID: AB_1549744) was used as the control. After incubation, the precipitates were collected by centrifugation, washed five times with the lysis buffer, and analyzed by immunoblotting (IB) using anti-FLAG antibody or anti-ANXA2 antibody. The same amount of purified recombinant FLAG-tagged YadC and ANXA2

protein were incubated in binding buffer (20 mM Tris-HCl (pH 7.4), 0.1% Triton-X 100, 100 mM NaCl, 20% glycerin, 1% BSA) for 12 h. The resulting complexes were then used to perform FLAG-tagged protein IP or ANXA2 protein IP, followed by immunoblotting.

2.12. Immunohistochemistry (IHC)

Bladder was fixed in 10% phosphate-buffered formalin for 48 h. The fixed tissue was then embedded in paraffin and cut into 5 μm sections. For immunohistochemistry analysis, sections were stained with anti-ANXA2 antibody (Proteintech, 11256-1-AP, 1:200). Images were acquired under a microscope (BX46, Olympus, Tokyo, Japan).

2.13. RNA interference

siRNAs for the targeted genes and a scrambled control siRNA (siScr) were synthesized by GenePharma (Shanghai, China). The siRNAs were transfected into 5637 cells using Lipofectamine 3000 (Invitrogen). Forty-eight hours post-transfection, the cells were analyzed for target protein expression by qRT-PCR and western blotting. The sequences of the siRNAs are listed in Table S2.

2.14. RNA extraction and qRT-PCR

RNA was extracted from siRNAs-transfected 5637 cells using a Total RNA Extraction Kit (Solarbio, Beijing, China) according to the manufacturer's protocol. RNA was converted to cDNA using a RevertAid First Strand cDNA Synthesis Kit (Thermo Scientific). β-actin was used as the endogenous control and data were normalized based on the transcription level of β-actin in the negative control and then analyzed using the comparative critical threshold cycle $2^{-\Delta\Delta Ct}$ method [37]. The primers used are listed in Table S2.

2.15. Western blotting

Whole cell lysates were prepared using RIPA lysis buffer (Millipore), with complete protease inhibitors (Roche, Basel, Switzerland). After estimating the protein concentration with BCA Protein Assay Kit (Thermo Fisher), 10−50 μg (per lane) of the cell lysates or co-immunoprecipitation (co-IP) products were subjected to SDS-PAGE and then blotted onto a polyvinylidene difluoride membrane (Millipore). The HRP conjugated anti-rabbit IgG (1:10000, Sigma-Aldrich) or anti-mouse IgG (1:10000, Sigma-Aldrich) were used to reveal antibody binding. Immunoreactive complexes were detected using Immobilon Western Chemiluminescent HRP Substrate (Millipore) and exposed to a GE Amersham Imager 600 machine.

2.16. ANXA2 inhibitor treatment

Compounds A-05 and A-07 were synthesized partially according to the protocol reported by Dekker and co-workers [38] and confirmed by ^{1}H NMR, ^{13}C NMR and HRMS (Supplementary Methods, Fig. S5). 5637 cells were treated with BAPTA-AM (5 μM) (Selleckchem, Houston, Texas, USA), compound A-05 (2.5 μM) or A-07 (1 μM) diluted in DMSO for 1 h, washed with PBS, then infected by UPEC for 1 h, and adhered and invaded bacteria were enumerated. For in vivo treatment, BAPTA-AM (2 mg/kg), compound A-05 (0.1 mg/kg), or DMSO were transurethrally injected into the bladder 1 h before bacterial infection, and mice were sacrificed at 24 hpi.

2.17. H&E staining

The bladders were fixed in 10% phosphate-buffered formalin for 48 h and embedded in paraffin. Sections (5 μm) were used for H&E staining. Images were acquired using a microscope (BX46, Olympus). For histopathology analysis, bladder inflammatory scores were determined blindly on H&E stained sections of bladders as previously described [39]. 0 = normal, 1 = subepithelial cell inflammatory infiltration (focal and multifocal), 2 = edema and subepithelial inflammatory cell infiltration (diffuse), 3 = marked subepithelial inflammatory cells with necrosis and neutrophils in and on bladder mucosal epithelium, 4 = inflammatory cell infiltrate extends into muscle in addition to criteria for grade 3, 5 = loss of surface epithelium (necrosis with full-thickness inflammatory cell infiltration).

2.18. Phylogenetic analysis

The MLST profile for each strain was assigned based on the nucleotide sequences of the seven housekeeping genes using MLST databases (http://mlst.warwick.ac.uk/mlst/) [40], and the sequences of the seven MLST genes from each strain were combined and used to construct the phylogenetic tree. A phylogenetic tree based on the alignments of DNA sequences was constructed using the maximum likelihood in MEGA 5 with 1000 bootstrap experiments [41].

2.19. Statistical analysis

Data are presented as the mean ± SD. The statistical significance of the differences between groups was calculated using a two-tailed Student's t-test, one-way ANOVA analysis or two-way ANOVA analysis of variance using the SPSS 20 software (IBM Corp., Aemonk, NY, USA). To analyze the bacterial titers in the UTI mouse models, the non-parametric Mann-Whitney test and the Kruskal−Wallis test were used to calculate the statistical significance.
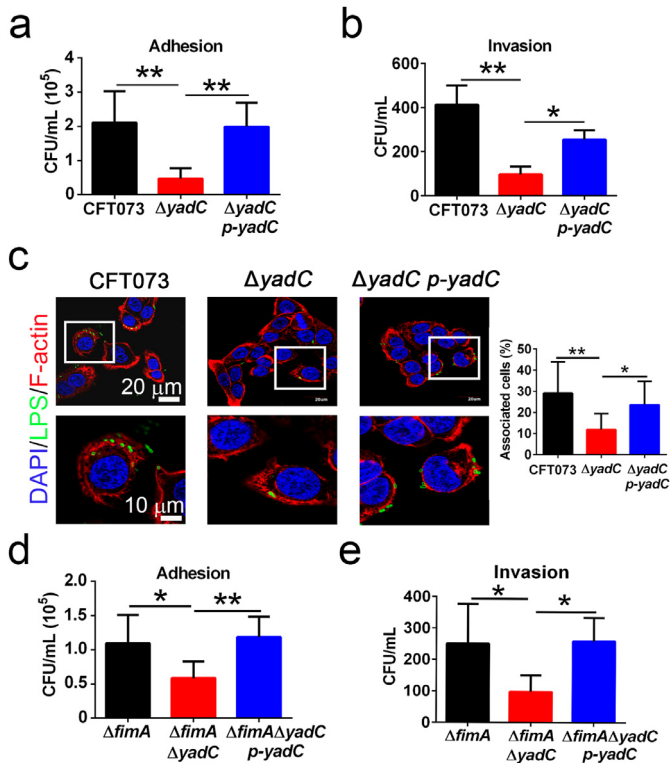
3. Results

3.1. YadC is involved in adhesion and invasion of UPEC to bladder epithelial cells

To study the role of YadC in UPEC adhesion and invasion to bladder epithelial cells, the UPEC wild-type strain CFT073, $\Delta yadC$ (deletion of $yadC$ gene), and $\Delta yadC$ p-yadC (the complemented strain) were used to infect bladder cell lines 5637 and T24. $\Delta yadC$ exhibited an attenuated ability to adhere and invade to 5637 and T24 compared with CFT073 and $\Delta yadC$ p-yadC (Figs. 1a, b and S1a−c). In immunofluorescence assays, the percentages of bladder cells associated with $\Delta yadC$ were reduced compared with those with CFT073 and $\Delta yadC$ p-yadC (Fig. 1c), while no difference was found for the motility of these strains (Fig. S1d). As type 1 fimbriae has been reported to play an important role in UPEC adhesion and invasion to bladder epithelial cells, we examined whether the effect of YadC depended on type 1 fimbriae. Based on the hemagglutination assays, the production of type 1 fimbriae was slightly decreased in both $\Delta yadC$ and $\Delta yadC$ p-yadC as compared with CFT073 (Table S3). In order to avoid the type 1 fimbriae effect, $\Delta fimA$ (deletion of the $fimA$ gene, which is involved in type 1 fimbriae assembly), $\Delta fimA\Delta yadC$ (deletion of both $fimA$ and $yadC$ genes), and $\Delta fimA\Delta yadC$ p-yadC strains, were constructed, and all these strains express no type 1 fimbriae (Table S3), and no significant difference was found for their motility (Fig. S1d). In adhesion and invasion assays, $\Delta fimA\Delta yadC$ showed decreased adhesion and invasion abilities (Figs. 1d, e and S1e). In addition, when we used 1% mannose to block type 1 fimbriae, the YadC effect was unchanged (Fig. S1f and g). These results indicate that YadC promotes UPEC adhesion and invasion to bladder epithelial cells independently of type 1 fimbriae.

3.2. YadC promotes UPEC colonization during acute bladder infections

To examine the role of YadC during acute UTIs, female C57BL/6J mice were transurethrally infected with 10^8 CFU of CFT073, $\Delta yadC$, or $\Delta yadC$ p-yadC strains, respectively. Bacterial titers in bladder infected by CFT073 or $\Delta yadC$ p-yadC at 12 and 24 hpi were obviously
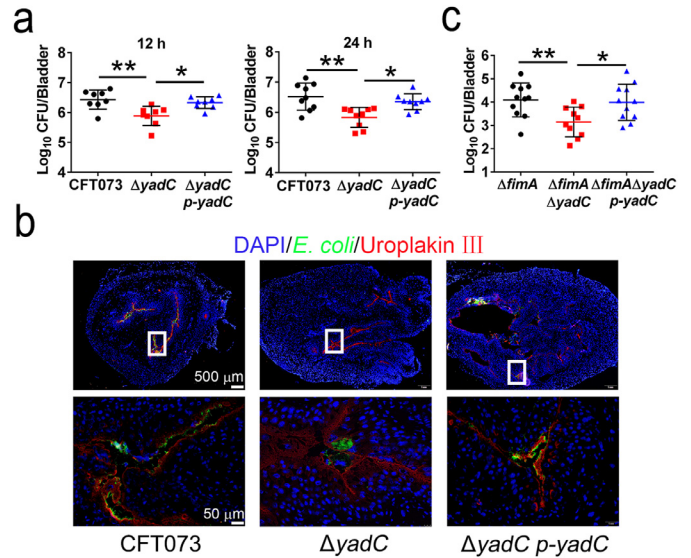
Fig. 1. YadC is involved in UPEC adhesion and invasion to bladder epithelial cells. Adhesion (a) and invasion (b) assays of CFT073, $\Delta yadC$ or $\Delta yadC$ p-yadC. 5637 cells were infected with bacteria at an MOI of 15 ($n = 3$). (c) Immunofluorescence analysis of 5637 cells infected with CFT073, $\Delta yadC$ or $\Delta yadC$ p-yadC at an MOI of 5 for 2 h ($n = 3$, three combined independent experiments each with four different fields). Blue, nucleus; Green, LPS; Red, F-actin. The percentage of associated cells was calculated by total bacteria-associated cells dividing total cells in all fields. Scale bar, 20 μm. Adhesion (d) and invasion (e) assays of $\Delta fimA$, $\Delta fimA\Delta yadC$, or $\Delta fimA\Delta yadC$ p-yadC. 5637 cells were infected with bacteria at an MOI of 50 ($n = 3$, three independent experiments). Data are the mean $\pm$ SD, one-way ANOVA, *$P < 0.05$, **$P < 0.01$.


Fig. 2. YadC promotes UPEC colonization during acute bladder infections.(a) Bacterial titers in the bladders of mice infected by CFT073, $\Delta yadC$, or $\Delta yadC$ p-yadC at 12 hpi ($n = 8$, two independent experiments) and 24 hpi ($n = 9$, three independent experiments). (b) Immunofluorescence analysis of bladder tissues at 24 hpi. Blue, nucleus; Green, E. coli; Red, Uroplakin III of bladder epithelial cells. Scale bar, 500 μm and 50 μm. (c) Bacterial titers in bladder of mice infected with $\Delta fimA$, $\Delta fimA\Delta yadC$ or $\Delta fimA\Delta yadC$ p-yadC at 24 hpi ($n = 10$ to 11, three independent experiments). Data are the mean $\pm$ SD, Kruskal–Wallis test, *$P < 0.05$, **$P < 0.01$.

higher than those in bladder infected by $\Delta yadC$ (Fig. 2a). Lower colonization of $\Delta yadC$ compared with CFT073 and $\Delta yadC$ p-yadC were also observed in immunofluorescence assays (Fig. 2b). In addition, bacterial titers in bladder infected by $\Delta fimA\Delta yadC$ were obviously lower than those by $\Delta fimA$ and $\Delta fimA\Delta yadC$ p-yadC (Fig. 2c). These results indicate that YadC promotes UPEC colonization in bladder, which is independently of type 1 fimbriae.

3.3. D-xylose targeting YadC has prophylactic and therapeutic effects on decreasing UPEC colonization

Binding of D-xylose to YadC, impedes E. coli K12 adhesion to intestinal epithelial cells [20]. As YadC plays an important role in UPEC colonization in bladder tissues, we hypothesized that D-xylose could be used as an anti-adhesion agent to prevent and treat UTIs. In the in vitro experiments, D-xylose reduced the bacterial titers of 5637 cells adhered and invaded by CFT073 or $\Delta yadC$ p-yadC without any effect on bacterial growth (Figs. 3a, b and S2a, b). However, D-xylose did not inhibit $\Delta yadC$ infection (Fig. 3a and b). Infection of bladder cells with three clinical UPEC strains was also inhibited by D-xylose (Fig. 3c). These results demonstrate that D-xylose impedes the association of UPEC with bladder cells by interacting with YadC.

We further investigated whether D-xylose had the prophylactic and therapeutic potential to treat UPEC infection in vivo. Female C57BL/6J mice were given 100 mg/kg D-xylose via oral gavage, and a D-xylose absorption test showed that the concentrations of D-xylose were highest in urine at 1 and 2 h after PO (per os) administration. The D-xylose concentrations were higher than 0.5 mg/ml (the

D-xylose concentration that had an effect in the in vitro experiments) from 1 to 5 h after treatment (Fig. 3d). The body weights of all animals were measured for a week after PO, and no apparent toxicity was observed, as measured by observable physiological changes, body weights, and survival (Fig. S2c). To examine the prophylactic effect of D-xylose, female C57BL/6J mice were orally administered with 100 mg/kg D-xylose or PBS at 30 min before transurethral inoculation with 10^8 CFU of CFT073, and bacterial titers in bladder tissues were determined at 3 hpi. To examine the therapeutic effect of D-xylose, mice were administered with 100 mg/kg D-xylose or PBS 3 h after CFT073 infection, and bacterial titers in bladder were determined after 4 h of administration. Significantly fewer bacteria were observed in mice treated with D-xylose compared with those treated with PBS (Fig. 3e, f). These results demonstrate that D-xylose has a potential to prevent and treat UPEC infection in mice.

3.4. ANXA2 is a receptor for YadC

To identify the YadC receptor in bladder epithelial cells, recombinant HA-tagged YadC was incubated with 5637 membrane-associated proteins, and the specific band detected using far-western blotting was identified as ANXA2 using LC-MS/MS (Fig. 4a). To confirm the interaction of YadC and ANXA2, co-immunoprecipitation assays were performed. After incubating with FLAG-tagged YadC for 12 h, 5637 cell lysates were immunoprecipitated with anti-FLAG or anti-ANXA2 antibody followed by immunoblotting with anti-ANXA2 or anti-FLAG antibody, respectively. The results showed that YadC was efficiently co-immunoprecipitated with endogenous ANXA2, and vice versa (Fig. 4b). To further verify the direct interaction between YadC and ANXA2, ANXA2 and FLAG-YadC proteins purified from E. coli strains were used to perform co-IP experiments, which showed direct interactions between YadC and ANXA2 (Fig. 4c). In immunofluorescence assays, ANXA2 was highly expressed in 5637 cells, and interestingly, YadC treatment induced the aggregation of ANXA2, and co-localization of YadC with endogenous ANXA2 was detected (Fig. 4d). Furthermore, ANXA2 was found colocalized with cell-associated bacteria (Fig. 4e). In addition, ANXA2 was highly
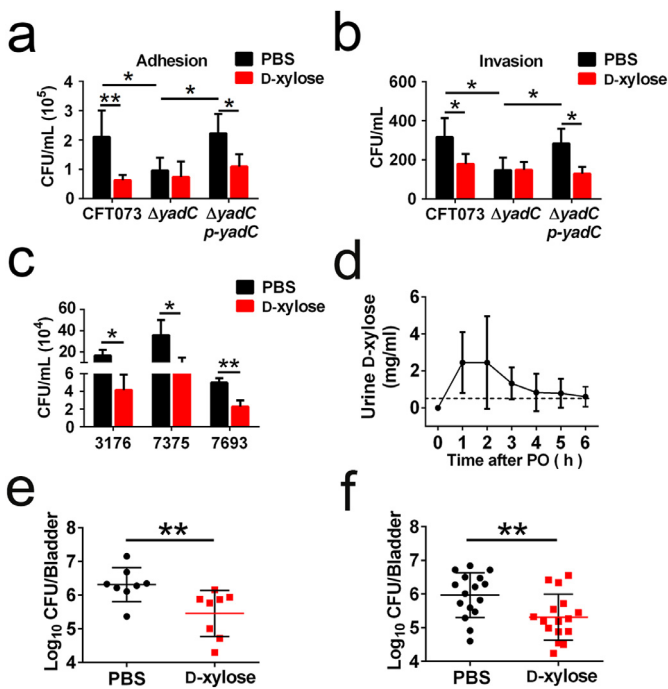
Fig. 3. D-xylose targeting YadC has the prophylactic and therapeutic effects on decreasing UPEC colonization. Adhesion (a) and invasion (b) assays of CFT073, ΔyadC or ΔyadC p-yadC. 5637 cells were infected with strains at an MOI of 15 in the presence of PBS or D-xylose (0.5 mg/ml), respectively (n = 3). (c) Bacteria associated with 5637 cells infected with three clinical UPEC strains at an MOI of 15 in the presence of PBS or D-xylose (0.5 mg/ml), respectively (n = 3). (d) The D-xylose concentration in urine of mice administered by oral gavage (100 mg/kg; PO, per os). The dotted line represents the D-xylose concentration (0.5 mg/ml) used in the in vitro assays. (e) Bacterial titers in bladder of mice orally administered with D-xylose (100 mg/kg) or PBS 30 min before transurethral inoculation with CFT073 (10^8 CFU). Bacterial titers were assessed at 3 hpi (n = 8, two independent experiments). (f) Bacterial titers in bladder of mice orally administered with D-xylose (100 mg/kg) or PBS 3 h after transurethral inoculation with CFT073 (10^8 CFU). Bacterial titers were assessed at 4 h after the administration of D-xylose or PBS (n = 16, three independent experiments). Data are the mean ± SD, two-way ANOVA (a, b), Student's t-test (c), or Mann−Whitney U test (e and f), *$P < 0.05$, **$P < 0.01$.

expressed in bladder epithelium, as analyzed by immunohistochemistry (Fig. S3a) and immunofluorescence assays (Fig. 4f), and UPEC appeared to be co-localized with ANXA2 in infected tissues (Fig. 4f). Taken together, these results indicate that ANXA2 is a receptor for YadC in bladder epithelial cells.

3.5. ANXA2 is involved in YadC-mediated UPEC infection of bladder epithelial cells

Next, we investigated whether ANXA2 is responsible for YadC-induced UPEC infection of bladder epithelial cells. Infection by CFT073 decreased significantly in 5637 cells transfected with siRNA targeting ANXA2 compared with that in cells transfected with a scrambled control siRNA; however, no difference was found upon ΔyadC infections between ANXA2 knockdown cells and control cells (Figs. 5a and S3b, c). BAPTA-AM is a cell permeable cytosolic calcium chelator without damage to cells [42]. As ANXA2 binds membrane phospholipids in a Ca2+-dependent manner [25], we used it as an inhibitor to impede ANXA2 function, as reported in other studies [32]. 5637 cells were treated with BAPTA-AM or DMSO for 1 h before infection with UPEC, and the adhesion and invasion of CFT073 or ΔyadC to cells were evaluated. In accordance with the results found in ANXA2 knockdown cells, inhibition of ANXA2 using BAPTA-AM decreased CFT073 infection but had no effect on ΔyadC infection (Fig. 5b, c), and BAPTA-AM had no effect on bacterial growth (Fig. S4a). Compounds reported to inhibit the ANXA2 and S100A10

interaction [38], were used to examine if they could inhibit YadC-mediated UPEC infection. Compounds A-05 and A-07, previously named as compound 35 and 37, were synthesized partially according to methods reported by Dekker (Fig. S5) [38], and were used to treat 5637 cells for 1 h before infection with CFT073 or ΔyadC. Compound A-05 or A-07 compared with DMSO significantly decreased adhesion and invasion of CFT073 but had no effect on that of ΔyadC (Fig. 5d, e). A-05 and A-07 also showed no effect on bacterial growth (Fig. S6a and b). These results show that YadC-mediated UPEC infection of bladder epithelial cells is dependent on its receptor ANXA2.

3.6. Inhibition of ANXA2 using BAPTA-AM or compound A-05 attenuates UPEC infection in vivo

To further confirm the role of ANXA2 in YadC-mediated UPEC infection in bladder, we evaluated effects of BAPTA-AM and compound A-05 on UPEC infection in vivo.

Female C57BL/6J mice were administered with 2 mg/kg BAPTA-AM or DMSO transurethrally 1 h before inoculation with 10^8 CFU of CFT073 or ΔyadC, and bacterial titers in bladder tissues were determined at 24 hpi. Significantly fewer bacteria were observed in the mice treated with BAPTA-AM compared with those treated with DMSO when infected with CFT073; however, no effect of BAPTA-AM was found for bacterial colonization when the mice were infected with ΔyadC (Fig. 5f). In addition, we examined the effect of BAPTA-AM on bladder tissue damage by H&E staining. The dose of BAPTA-AM used did not destroy the structure and integrity of bladder epithelial cells without infection as shown by H&E staining (Fig. S4b). BAPTA-AM treatment obviously decreased edema and infiltrated immune cells induced by CFT073 infection; however, it had no effect on bladder tissues infected with ΔyadC (Fig. 5g).

Female C57BL/6J mice were transurethrally administered with 0.1 mg/kg compound A-05 or DMSO 1 h before infected with 10^8 CFU of CFT073 or ΔyadC. CFT073 colonization was decreased in mice treated with compound A-05 compared with those treated with DMSO (Fig. 5h). However, ΔyadC infection was not affected by compound A-05 (Fig. 5h). Compound A-05 decreased edema and infiltrated immune cells in bladder tissues infected by CFT073 in H&E staining analysis (Fig. 5i), but it did not induce bladder damage without infection (Fig. S6c). In addition, the effect of compound A-05 on infections by UTI89 (another UPEC strain commonly used) or UTI89 ΔyadC (yadC deletion strain derived from UTI89) was also examined, and results similar to those for CFT073 were obtained (Fig. S6d and e).

3.7. The yadC gene is widely present in UPEC strains

Among the 63 UPEC strains with available genome sequences, we found that 47 strains harbored a yadC gene [5]. A phylogenetic tree was constructed based on the alignment of these yadC sequences, and these yadC were divided into six subgroups (Fig. 6a). The major topology of the tree based on yadC was very similar to that of the tree based on MLST genes of these 47 strains, implying that yadC is conserved as the housekeeping MLST genes (Fig. 6a and b). The yadC gene was also found in 27 clinical UPEC isolates and was sequenced. The yadC sequences from the clinical strains and those from the representative strains (CFT073, UTI89, 11, Ec958, 4, 7) of the six separated subgroups were used to construct a phylogenetic tree. The clinical yadC sequences were separated into seven subgroups, with 85% belonging to the six subgroups, indicating that yadC is widely present in UPEC clinical strains and is conserved to maintain its function (Fig. 6c).

4. Discussion

In this study, YadC, the tip-adhesin of Yad fimbriae, was identified to be important for UPEC infection of bladder epithelial cells in vitro and colonization in bladder during acute UTIs in vivo.
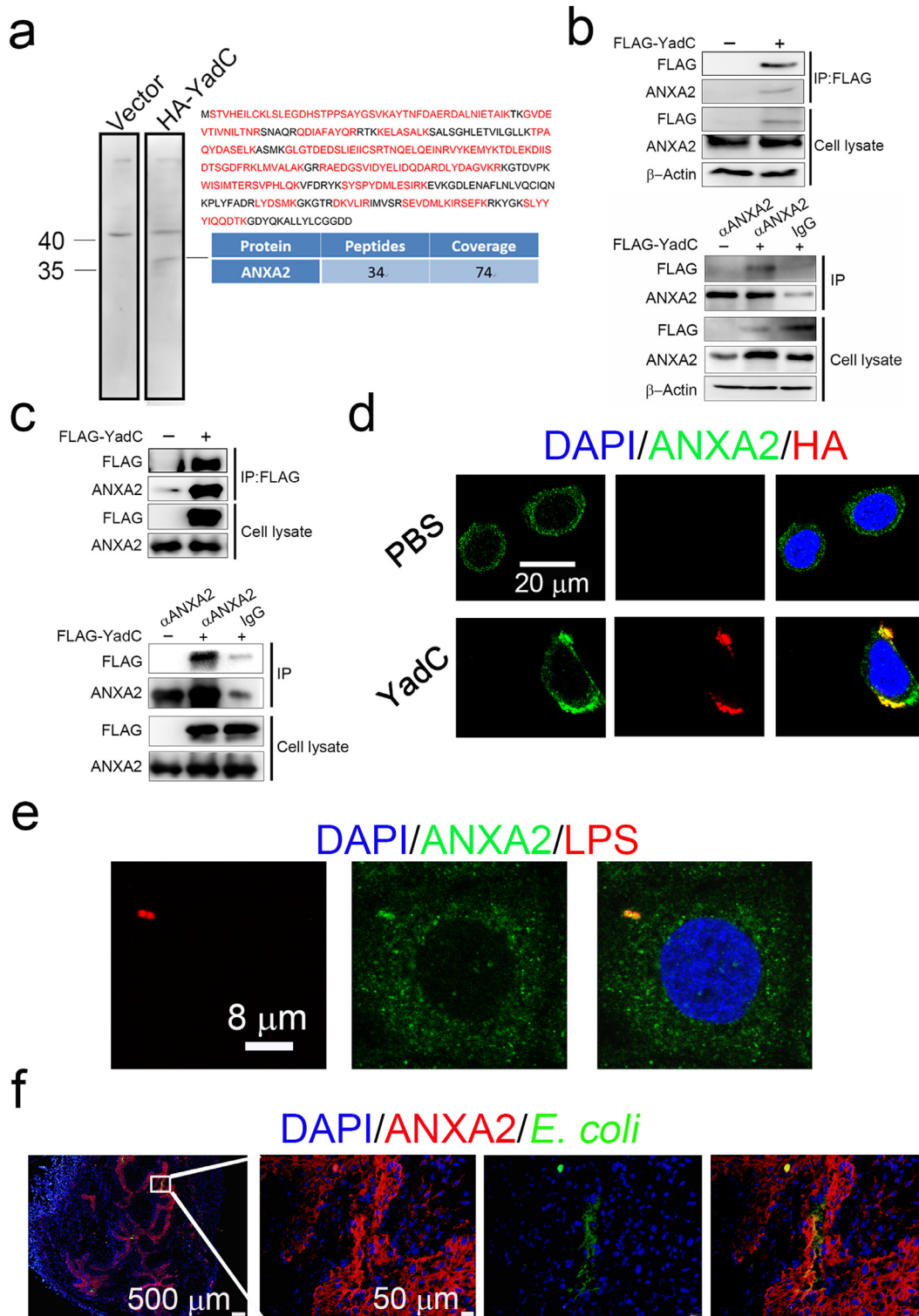
Fig. 4. ANXA2 is a receptor for YadC.(a) Analysis of 5637 cell membrane proteins binding to HA-YadC by far western blotting and LC-MS/MS. The peptides detected and peptide coverage percentage of ANXA2 are shown. Detected peptides belonging to ANXA2 are indicated in red. (b) Co-immunoprecipitation analysis of the interaction between FLAG-YadC with ANXA2 in 5637 cells. α, anti-. (c) Co-immunoprecipitation analysis of the interaction between the purified ANXA2 and FLAG-YadC protein. (d) Immunofluorescence analysis of ANXA2 and HA-YadC localization in 5637 cells. Blue, nucleus; Green, ANXA2; Red, HA. Scale bar, 20 μm. (e) Immunofluorescence analysis of ANXA2 and E. coli localization in 5637 cells. Blue, nucleus; Red, LPS; Green, ANXA2. Scale bar, 8 μm. (f) Immunofluorescence analysis of ANXA2 and E. coli localization in mouse bladder tissue infected with CFT073. Blue, nucleus; Green, E. coli; Red, ANXA2. Scale bar, 500 μm and 50 μm.

Since Yad fimbriae is present in most UPEC isolates like type 1 fimbriae, we believe that YadC plays an important role in UPEC pathogenicity.

Due to deficiencies in antibiotic treatment of UTI, non-antibiotic therapeutics are necessary to be developed. Much attention has been focused on the anti-adhesion therapy targeting the fimbrial adhesins responsible for UPEC colonization. The most well-developed anti-adhesion therapy is based on FimH, the tip-adhesin of type 1 fimbriae. Mannose and its derivatives (mannosides), targeting FimH, have been proved to interrupt the binding and colonization of UPEC
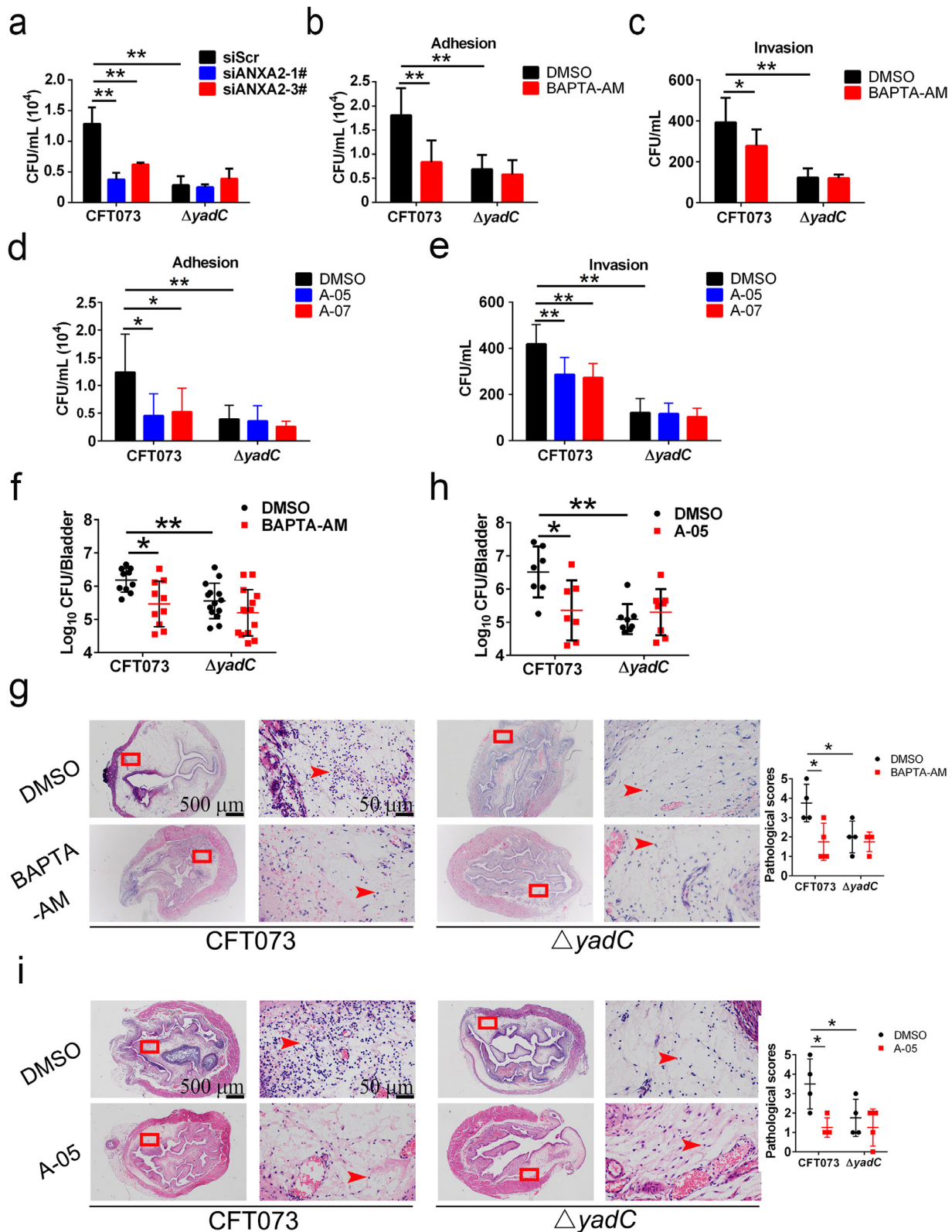
Fig. 5. ANXA2 is involved in YadC-mediated UPEC infection.(a) Associated bacteria in 5637 cells transfected with scrambled siRNA or siRNA targeting ANXA2 and infected with CFT073 or $\Delta yadC$ in serum-free RMPI 1640 (n = 3). Adhesion (b) and invasion (c) assays of bacteria to 5637 cells treated with BAPTA-AM (5 μM) or DMSO for 1 h and infected with CFT073 or $\Delta yadC$ in serum-free RMPI 1640 (n = 3). Adhesion (d) and invasion (e) assays of bacteria to 5637 cells treated with compounds A-05 (2.5 μM), A-07 (1 μM), or DMSO for 1 h and infected with CFT073 or $\Delta yadC$ in serum-free RMPI 1640 (n = 3). Cells were infected with bacteria at an MOI of 15 for 1 h. Data are the mean ± SD, two-way ANOVA, *P < 0.05, **P < 0.01. Bacterial titers in bladder (f) or representative images of H&E staining of bladder tissues (g) of mice transurethrally administered with BAPTA-AM (2 mg/kg) or DMSO 1 h before transurethral inoculation with CFT073 or $\Delta yadC$ (10^8 CFU). Bacterial titers were assessed at 24 hpi (n = 10 to 14, three independent experiments). Pathological scores are shown in the right (n = 4, three independent experiments). Bacterial titers in bladder (h) or representative images of H&E staining of bladder tissues (i) of mice transurethrally administered with compound A-05 (0.1 mg/kg) or DMSO 1 h before transurethral inoculation with CFT073 or $\Delta yadC$ (10^8 CFU, n = 7 to 8, three independent experiments). Pathological scores are shown in the right (n = 4, three independent experiments). Scale bar, 500 μm and 50 μm. Data are mean ± SD. Mann–Whitney U test. *P < 0.05, **P < 0.01.
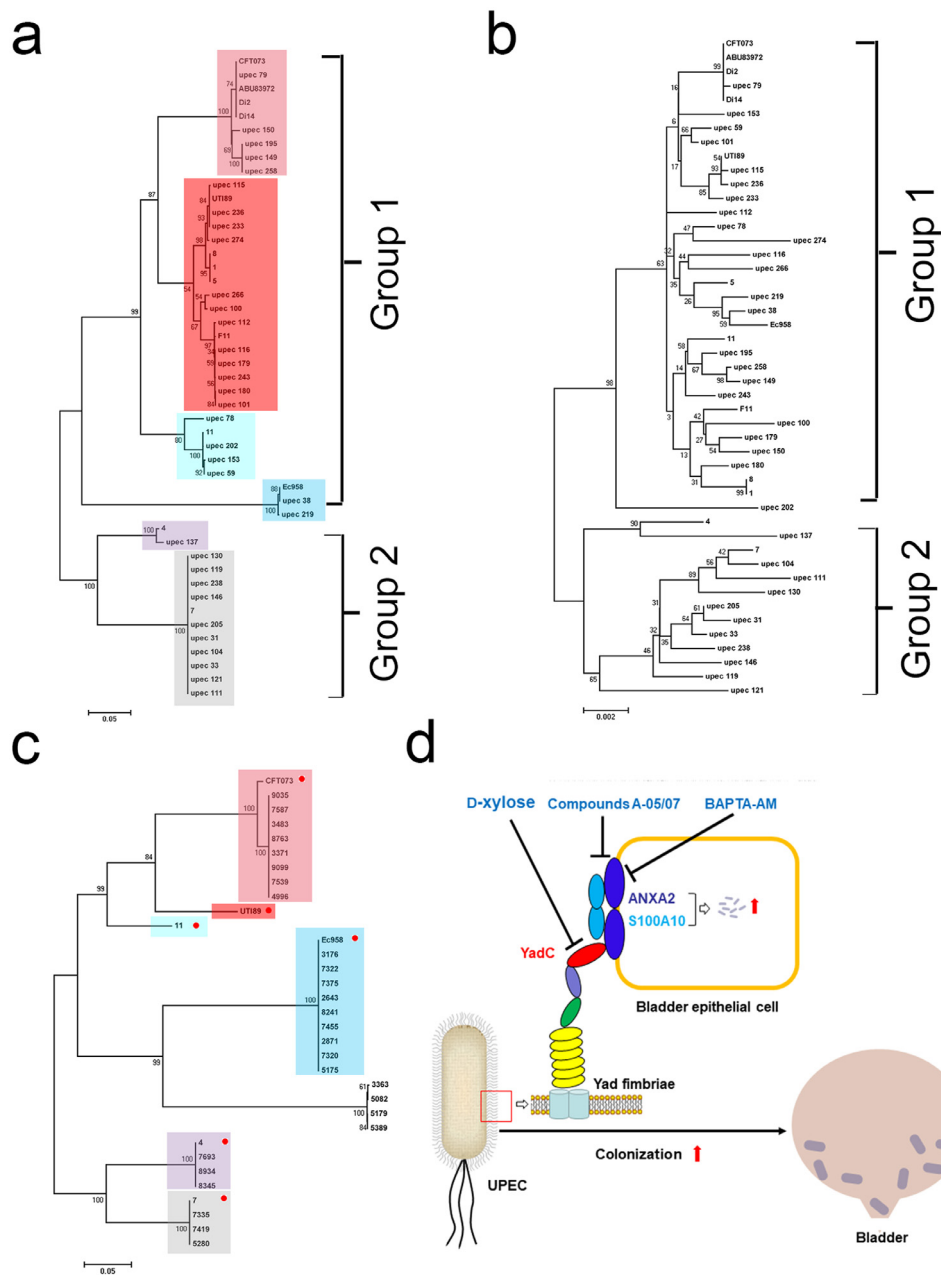
Fig. 6. Phylogenetic analysis of *yadC*.Phylogenetic trees of 47 UPEC strains with available genome sequences based on *yadC* (a) and MLST (b). Rectangles with different colors indicate different subgroups separated in the tree. (c) A phylogenetic tree of 27 clinical UPEC isolates and the representative strains (CFT073, UTI89, 11, Ec958, 4, and 7, indicated by red circles) of the six separated subgroups in (a). Rectangles with different colors indicate the corresponding subgroups in (a). The scales at the bottoms of the trees indicate the phylogenetic distance. Bootstrap values are displayed as percentages on the nodes (a−c). (d) Schematic diagram of YadC-mediated acute bladder infections and three treatment strategies.

in bladder, thereby attenuating the virulence of UPEC. Most UPEC strains express multiple types of fimbriae during infection, and anti-adhesion therapy including multiple agents targeting different fimbriae will be more effective. Therefore, it is indispensable to develop anti-adhesion agents for other types of fimbrial adhesins. Identification of different fimbriae and their receptors on host cells, involved in UPEC colonization, is necessary to develop anti-adhesion therapy.

D-xylose was reported to bind to YadC [20]. In this study, we found that D-xylose inhibited YadC-mediated UPEC infection of bladder epithelial cells and colonization in bladder in vivo. D-xylose is a natural pentose sugar abundant in corn cobs, coconuts, seed hulls, and straw [43]. D-xylose supplements are beneficial for postprandial glycemic responses in subjects with normal glucose levels and patients with prediabetes [44]. D-xylose also improved serum lipids

and attenuated lipid accumulation in the livers of high-fat diet-induced obese mice [45]. D-xylose has been used as sweetener because of its incomplete absorption [46]. In the intestine, D-xylose can selectively promote the proliferation of probiotics such as *Bifido-bacterium*, making them to dominant intestinal flora, which could regulate intestinal micro-ecological balance and promote intestinal health [47]. However, the amount and potential adverse effects for D-xylose to treat and prevent human UTIs should be taken into consideration and carefully evaluated in further studies. In addition, whether treatment targeting YadC could enhance the therapy based on FimH should also be considered.

ANXA2 was identified as a potential receptor for bacteria such as *Pseudomonas aeruginosa* [28] and viruses such as respiratory syncytial virus (RSV) [29]. ANXA2 is also reported to be responsible for several viral and

bacterial infections of epithelial cells, including human papillomaviruses (HPV), HCV, HIV, EHEC and *Salmonella Typhimurium* [30, 31, 48–50]. We found that ANXA2 was a receptor for YadC on bladder epithelial cells. YadC could bind to ANXA2 directly, and the ANXA2 is involved in YadC-mediated UPEC infection of bladder epithelial cells. Therefore, ANXA2 in epithelial cells could be a therapeutic target for acute UTIs.

BAPTA-AM, as a cytosolic calcium chelator inducing no cell damage, can prevent ethanol-induced locomotory stimulation without altered basal locomotion, reverse ethanol-induced hypnotic effects in Swiss mice and reduce ethanol consumption in male C57BL/6J mice [51]. In addition, BAPTA-AM nanoparticles have a renal-protective role in ischemia/reperfusion induced acute kidney injury [52]. We found that BAPTA-AM could decrease UPEC infection and colonization in bladder during acute UTIs. ANXA2 is reported to be involved in bacterial and viral infections by binding to S100A10, such as promoting cryptococcal transcytosis across the BMECs [32] and HPV internalization in epithelial cells [30]. We found that two compounds inhibiting the ANXA2-S100A10 interaction impeded YadC-mediated UPEC infection, indicating that YadC promotes UPEC infection depending on the binding of ANXA2 to S100A10; however, the specificity of the compounds need to be examined in further studies. Taken together, compounds targeting YadC, ANXA2, or the interactions between ANXA2 and S100A10 have the potential to treat acute UTIs (Fig. 6d).

Declaration of Competing Interest

The authors have no potential conflicts of interest to disclose.

CRediT authorship contribution statement

Xiao Li: Data curation, Formal analysis, Investigation, Methodology, Validation, Writing - original draft. **Geng Pei:** Data curation, Formal analysis, Investigation, Validation, Methodology. **Lisong Zhang:** Investigation, Methodology. **Yang Cao:** Resources, Investigation. **Jingyu Wang:** Investigation, Methodology. **Lu Yu:** Investigation, Methodology. **Wei Dianjun:** Resources, Investigation. **Shan Gao:** Investigation, Methodology. **Zhi-Song Zhang:** Resources, Investigation, Methodology. **Zhi Yao:** Resources. **Quan Wang:** Data curation, Formal analysis, Project administration, Resources, Supervision, Writing - review & editing.

Acknowledgments

Abbreviations qRT-PCR: Quantitative reverse transcription PCR; LC-MS/MS: Liquid chromatography-tandem mass spectrometry; DMSO: Dimethyl sulfoxide; LPS: Lipopolysaccharide; IPTG: Isopropyl β-D-1-thiogalactopyranoside; H&E: Hematoxylin and eosin; OCT: Optimal cutting temperature compound; BSA: Bovine serum albumin; DAPI: 2-(4-amidinophenyl)-1H-indole-6-carboxamidine; MOI: Multiplicity of infection; siRNAs: Short interfering RNAs; ANOVA: Analysis of variance.

Supplementary materials

Supplementary material associated with this article can be found, in the online version, at doi:10.1016/j.ebiom.2019.11.014.

References

[1] Nielubowicz GR, Mobley HL. Host-pathogen interactions in urinary tract infection. Nat Rev Urol 2010;7:430–41.

[2] Kucheria R, Dasgupta P, Sacks SH, Khan MS, Sheerin NS. Urinary tract infections: new insights into a common problem. Postgrad Med J 2005;81:83–6.

[3] Hunstad DA, Justice SS. Intracellular lifestyles and immune evasion strategies of uropathogenic *Escherichia coli*. Annu Rev Microbiol 2010;64:203–21.

[4] Dhakal BK, Kulesus RR, Mulvey MA. Mechanisms and consequences of bladder cell invasion by uropathogenic *Escherichia coli*. Eur J Clin Invest 2008;38(Suppl 2):2–11.

[5] Ren Y, Palusiak A, Wang W, Wang Y, Li X, Wei H, et al. A high-resolution typing assay for uropathogenic *Escherichia coli* based on fimbrial diversity. Front Microbiol 2016;7:623.

[6] Wright KJ, Seed PC, Hultgren SJ. Development of intracellular bacterial communities of uropathogenic *Escherichia coli* depends on type 1 pili. Cell Microbiol 2007;9:2230–41.

[7] Lane MC, Mobley HL. Role of P-fimbrial-mediated adherence in pyelonephritis and persistence of uropathogenic *Escherichia coli* (UPEC) in the mammalian kidney. Kidney Int 2007;72:19–25.

[8] Proft T, Baker EN. Pili in gram-negative and gram-positive bacteria − structure, assembly and their role in disease. Cell Mol Life Sci 2009;66:613–35.

[9] Eto DS, Jones TA, Sundsbak JL, Mulvey MA. Integrin-mediated host cell invasion by Type 1-piliated uropathogenic *Escherichia coli*. PLoS Pathog 2007;3:e100.

[10] Zhou G, Mo WJ, Sebbel P, Min G, Neubert TA, Glockshuber R, et al. Uroplakin IA is the urothelial receptor for uropathogenic *Escherichia coli*: evidence from in vitro FimH binding. J Cell Sci 2001;114:4095–103.

[11] Flores-Mireles AL, Walker JN, Caparon M, Hultgren SJ. Urinary tract infections: epidemiology, mechanisms of infection and treatment options. Nat Rev Microbiol 2015;13:269–84.

[12] Mike LA, Smith SN, Sumner CA, Eaton KA, Mobley HL. Siderophore vaccine conjugates protect against uropathogenic *Escherichia coli* urinary tract infection. Proc Natl Acad Sci USA 2016;113:13468–73.

[13] Sivick KE, Mobley HL. Waging war against uropathogenic *Escherichia coli*: winning back the urinary tract. Infect Immun 2010;78:568–85.

[14] Cusumano CK, Pinkner JS, Han Z, Greene SE, Ford BA, Crowley JR, et al. Treatment and prevention of urinary tract infection with orally active FimH inhibitors. Sci Transl Med 2011;3:109ra115.

[15] Ohlsson J, Jass J, Uhlin BE, Kihlberg J, Nilsson UJ. Discovery of potent inhibitors of PapG adhesins from uropathogenic *Escherichia coli* through synthesis and evaluation of galabiose derivatives. Chembiochem 2002;3:772–9.

[16] Wurpel DJ, Beatson SA, Totsika M, Petty NK, Schembri MA. Chaperone-usher fimbriae of *Escherichia coli*. PLoS One 2013;8:e52835.

[17] Dziva F, Hauser H, Connor TR, van Diemen PM, Prescott G, Langridge GC, et al. Sequencing and functional annotation of avian pathogenic *Escherichia coli* serogroup O78 strains reveal the evolution of *E. coli* lineages pathogenic for poultry via distinct mechanisms. Infect Immun 2013;81:838–49.

[18] Verma R, Rojas TC, Maluta RP, Leite JL, da Silva LP, Nakazato G, et al. Fimbria-encoding gene *yadC* has a pleiotropic effect on several biological characteristics and plays a role in avian pathogenic *Escherichia coli* pathogenicity. Infect Immun 2016;84:187–93.

[19] Spurbeck RR, Stapleton AE, Johnson JR, Walk ST, Hooton TM, Mobley HL. Fimbrial profiles predict virulence of uropathogenic *Escherichia coli* strains: contribution of Ygi and Yad fimbriae. Infect Immun 2011;79:4753–63.

[20] Larsonneur F, Martin FA, Mallet A, Martinez-Gil M, Semetey V, Ghigo JM, et al. Functional analysis of *Escherichia coli* Yad fimbriae reveals their potential role in environmental persistence. Environ Microbiol 2016;18:5228–48.

[21] Schuliga M, Royce SG, Langenbach S, Berhan A, Harris T, Keenan CR, et al. The coagulant factor Xa induces protease-activated receptor-1 and annexin A2-dependent airway smooth muscle cytokine production and cell proliferation. Am J Respir Cell Mol Biol 2016;54:200–9.

[22] de Graauw M, Cao L, Winkel L, van Miltenburg MH, le Devedec SE, Klop M, et al. Annexin A2 depletion delays EGFR endocytic trafficking via cofilin activation and enhances EGFR signaling and metastasis formation. Oncogene 2014;33:2610–9.

[23] Moreau K, Ghislat G, Hochfeld W, Renna M, Zavodszky E. Transcriptional regulation of Annexin A2 promotes starvation-induced autophagy. Nat Commun 2015;6:8045.

[24] Urbanska A, Sadowski L, Kalaidzidis Y, Miaczynska M. Biochemical characterization of APPL endosomes: the role of annexin A2 in APPL membrane recruitment. Traffic 2011;12:1227–41.

[25] Moss SE, Morgan RO. The annexins. Genome Biol 2004;5:219.

[26] Gerke V, Moss SE. Annexins: from structure to function. Physiol Rev 2002;82: 331–71.

[27] Liu Y, Myrvang HK, Dekker LV. Annexin A2 complexes with S100 proteins: structure, function and pharmacological manipulation. Br J Pharmacol 2015;172:1664–76.

[28] Kirschnek S, Adams C, Gulbins E. Annexin II is a novel receptor for *Pseudomonas aeruginosa*. Biochem Biophys Res Commun 2005;327:900–6.

[29] Malhotra R, Ward M, Bright H, Priest R, Foster Martyn R, Hurle M, et al. Isolation and characterisation of potential respiratory syncytial virus receptor(s) on epithelial cells. Microbes Infect 2003;5:123–33.

[30] Woodham AW, Da Silva DM, Skeate JG, Raff AB, Ambroso MR, Brand HE, et al. The S100A10 subunit of the annexin A2 heterotetramer facilitates L2-mediated human papillomavirus infection. PLoS One 2012;7:e43519.

[31] Jolly C, Winfree S, Hansen B, Steele-Mortimer O. The Annexin A2/p11 complex is required for efficient invasion of *Salmonella Typhimurium* in epithelial cells. Cell Microbiol 2014;16:64–77.

[32] Fang W, Fa ZZ, Xie Q, Wang GZ, Yi J, Zhang C, et al. Complex roles of Annexin A2 in host blood-brain barrier invasion by *Cryptococcus neoformans*. CNS Neurosci Ther 2017;23:291–300.

[33] Datsenko KA, Wanner BL. One-step inactivation of chromosomal genes in *Escherichia coli* K-12 using PCR products. Proc Natl Acad Sci USA 2000;97:6640–5.

[34] Hung CS, Dodson KW, Hultgren SJ. A murine model of urinary tract infection. Nat Protoc 2009;4:1230–43.

[35] Eberts TJ, Sample RH, Glick MR, Ellis GH. A simplified, colorimetric micromethod for xylose in serum or urine, with phloroglucinol. Clin Chem 1979;25:1440–3.

[36] Wu Y, Li Q, Chen XZ. Detecting protein-protein interactions by Far western blotting. Nat Protoc 2007;2:3278–84.

[37] Livak KJ, Schmittgen TD. Analysis of relative gene expression data using real-time quantitative PCR and the 2(-Delta Delta C(T)) method. Methods 2001;25:402–8.

[38] Reddy TR, Li C, Guo X, Fischer PM, Dekker LV. Design, synthesis and SAR exploration of tri-substituted 1,2,4-triazoles as inhibitors of the annexin A2-S100A10 protein interaction. Bioorg Med Chem 2014;22:5378–91.

[39] Hopkins WJ, Gendron-Fitzpatrick A, Balish E, Uehling DT. Time course and host responses to *Escherichia coli* urinary tract infection in genetically distinct mouse strains. Infect Immun 1998;66:2798–802.

[40] Tartof SY, Solberg OD, Manges AR, Riley LW. Analysis of a uropathogenic *Escherichia coli* clonal group by multilocus sequence typing. J Clin Microbiol 2005;43:5860–4.

[41] Tamura K, Peterson D, Peterson N, Stecher G, Nei M, Kumar S. MEGA5: molecular evolutionary genetics analysis using maximum likelihood, evolutionary distance, and maximum parsimony methods. Mol Biol Evol 2011;28:2731–9.

[42] Son SM, Byun J, Roh SE, Kim SJ, Mook-Jung I. Reduced IRE1alpha mediates apoptotic cell death by disrupting calcium homeostasis via the InsP3 receptor. Cell Death Dis 2014;5:e1188.

[43] Bae YJ, Bak YK, Kim B, Kim MS, Lee JH, Sung MK. Coconut-derived D-xylose affects postprandial glucose and insulin responses in healthy individuals. Nutr Res Pract 2011;5:533–9.

[44] Jun YJ, Lee J, Hwang S, Kwak JH, Ahn HY, Bak YK, et al. Beneficial effect of xylose consumption on postprandial hyperglycemia in Korean: a randomized double-blind, crossover design. Trials 2016;17:139.

[45] Lim E, Lim JY, Shin JH, Seok PR, Jung S, Yoo SH, et al. D-Xylose suppresses adipogenesis and regulates lipid metabolism genes in high-fat diet-induced obese mice. Nutr Res 2015;35:626–36.

[46] Seri K, Sanai K, Matsuo N, Kawakubo K, Xue C, Inoue S. L-arabinose selectively inhibits intestinal sucrase in an uncompetitive manner and suppresses glycemic response after sucrose ingestion in animals. Metabolism 1996;45:1368–74.

[47] Liu D, Wang S, Xu B, Guo Y, Zhao J, Liu W, et al. Proteomics analysis of *Bifidobacterium longum* NCC2705 growing on glucose, fructose, mannose, xylose, ribose, and galactose. Proteomics 2011;11:2628–38.

[48] Saxena V, Lai CK, Chao TC, Jeng KS, Lai MM. Annexin A2 is involved in the formation of hepatitis C virus replication complex on the lipid raft. J Virol 2012;86: 4139–50.

[49] Ma G, Greenwell-Wild T, Lei K, Jin W, Swisher J, Hardegen N, et al. Secretory leukocyte protease inhibitor binds to annexin II, a cofactor for macrophage HIV-1 infection. J Exp Med 2004;200:1337–46.

[50] Tobe T. Cytoskeleton-modulating effectors of enteropathogenic and enterohemorrhagic *Escherichia coli*: role of EspL2 in adherence and an alternative pathway for modulating cytoskeleton through Annexin A2 function. FEBS J 2010;277: 2403–8.

[51] Balino P, Monferrer L, Pastor R, Aragon CM. Intracellular calcium chelation with BAPTA-AM modulates ethanol-induced behavioral effects in mice. Exp Neurol 2012;234:446–53.

[52] He Z, Tang H, You X, Huang K, Dhinakar A, Kang Y, et al. BAPTA-AM nanoparticle for the curing of acute kidney injury induced by ischemia/reperfusion. J Biomed Nanotechnol 2018;14:868–83.